CHARACTERISTIC SURFACES FOR THREE-POSITION MOTION GENERATION WITH PLANAR FOUR-BAR MECHANISMS.

Clark R. Barker
Missouri University of Science and Technology

J. Baumann

CHARACTERISTIC SURFACES FOR THREE POSITION FUNCTION GENERATION WITH PLANAR FOUR BAR MECHANISMS

C. R. Barker and P. -L. Tso
University of Missouri-Rolla
Mechanical and Aerospace Engineering Department
Rolla, Missouri

ABSTRACT

This paper considers the relationship between the three position function generation problem and the solution space for planar four bar mechanisms. The two infinities of solutions possible are mapped in a plane to determine the locations where particular types of mechanisms occur. It is possible to generate a contour in the mapping plane which joins together all solutions which possess a common characteristic in regard to their link lengths. This same contour can be displayed in the solution space to ascertain the overall characteristics of potential solutions to the design problem. A numerical example is used for illustrative purposes, but the results can be applied to any three position function generation problem.

INTRODUCTION

In the synthesis of planar four bar mechanisms, the use of three design or precision positions is often considered. Limiting the number of finitely separated positions to three has the advantage of providing the designer with a large number of potential solutions to the synthesis problem. This on the other hand makes the selection of the one final choice more difficult unless additional information is provided which makes it possible to eliminate the large number of undesirable solutions which occur.

Recently Barker [1] has proposed a classification scheme for planar four bar mechanisms which is based upon a solution space concept. He has shown that properties such as transmission angle, range of travel of the links, maximum and minimum angular velocity ratios, etc [2,3,4] can be conveniently represented by characteristic surfaces in planes of the solution space. The trace of these surfaces in planes of the solution space provides considerable information to the designer regarding the properties of the potential solutions of the design problem.

The intent of this work is to show that similar surfaces exist for the three position function generation problem, and that as a result all of the previous work can be applied to the present synthesis task. Considered first will be the generation of a mapping of all possible solutions to the three position function generation problem. The map will represent the two infinities of solutions which exist for a chosen numerical example, and it will indicate where each type of planar four bar solution can be found according to the classification of Ref. 1. Next the generation of all possible solutions to the problem which posses a common characteristic with regard to the lengths of the links will be considered. The results will be displayed both in the plane of the mapping and in the solution space.

PREVIOUS WORK ON MAPPING FOR THREE PRECISION POINTS

The value of mapping the large number of solutions to a three precision point problem has been recognized by other researchers. Waldron & Strong [5] map areas corresponding to the rotation properties of links and joints of dyads using geometric techniques. Gupta [6] mapped areas where crank-rocker function generators exist and meet certain transmission angle requirements. Recently Harber, Erdman, and Riley [7,8] have used mappings in conjunction with the work of Barker [1] to enhance the Lincages package for the case of three design position synthesis.

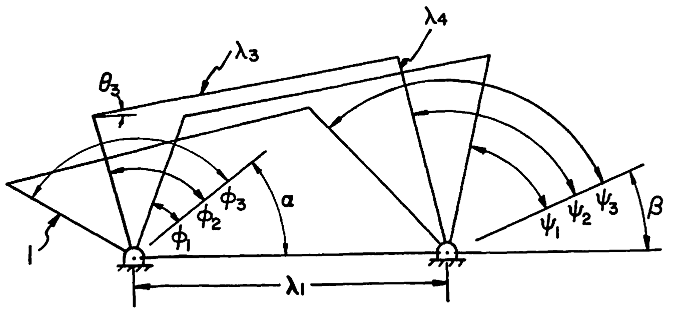

Fig. 1 Basic Arrangement for Three Position Function Generation

BASIC EQUATIONS FOR THREE PRECISION POINTS

Fig. 1 shows the basic arrangement for a three position function generation problem. The length of the input link is taken to be unity and the frame, coupler, and output link lengths are λ_1, λ_3, and λ_4 respectively. The angles α and β define reference positions from which the angles ϕ and ψ are to be measured. The angles ϕ_1, ϕ_2, and ϕ_3 and ψ_1, ψ_2, and ψ_3 are the desired coordinated positions to be achieved in the synthesis and their values are assumed to be known. Using the position vector loop approach for any of the three desired positions leads to the equations

$$\cos(\alpha+\phi_n)+\lambda_3 \cos\theta_{3n} = \lambda_1+\lambda_4 \cos(\beta+\psi_n) \tag{1}$$

$$\sin(\alpha+\phi_n)+\lambda_3 \sin\theta_{3n} = \lambda_4 \sin(\beta+\psi_n) \quad \text{for } n = 1,\ 2, \text{ or } 3.$$

Eliminating the angle θ_{3n} of the coupler leads to a result given by Freudenstein in Ref. [9] where

$$\begin{aligned} K_1 \cos(\phi_1+\alpha)+K_2 \cos(\psi_1+\beta)+K_3 &= -\cos(\phi_1+\alpha-\psi_1-\beta) \\ K_1 \cos(\phi_2+\alpha)+K_2 \cos(\psi_2+\beta)+K_3 &= -\cos(\phi_2+\alpha-\psi_2-\beta) \\ K_1 \cos(\phi_3+\alpha)+K_2 \cos(\psi_3+\beta)+K_3 &= -\cos(\phi_3+\alpha-\psi_3-\beta) \end{aligned} \tag{2}$$

with $\quad K_1 = \lambda_1/\lambda_4 \qquad K_2 = -\lambda_1$

and $\quad K_3 = (\lambda_3^2 - \lambda_1^2 - \lambda_4^2 - 1)/2\lambda_4$.

Using the notation

$$\begin{aligned} A_n &= \cos(\phi_n+\alpha) \\ B_n &= \cos(\psi_n+\beta) \\ C_n &= \cos(\phi_n+\alpha-\psi_n-\beta) \\ &\text{For } n = 1,\ 2,\ 3 \end{aligned} \tag{3}$$

it is possible to eliminate K_3 from Eq. (2) and then solve for K_1 and K_2. The result is

$$K_1 = \lambda_1/\lambda_4 = \text{NUM1/DENOM} \qquad K_2 = -\lambda_1 = -\text{NUM2/DENOM} \tag{4}$$

where

$$\begin{aligned} \text{NUM1} &= (B_1-B_2)(C_2-C_3)-(B_2-B_3)(C_1-C_2) \\ \text{NUM2} &= (A_1-A_2)(C_2-C_3)-(A_2-A_3)(C_1-C_2) \\ \text{DENOM} &= (A_1-A_2)(B_2-B_3)-(A_2-A_3)(B_1-B_2). \end{aligned} \tag{5}$$

For a given choice of α and β and known values of ϕ_n and ψ_n, it is therefore possible to calculate K_1, K_2, and K_3 and then find λ_1, λ_3, and λ_4. The calculations are straightforward except for twelve special locations where the values of K_1 and K_2 given by Eq. (4) assume the indeterminate form 0/0. Let the values

$$\begin{aligned} \gamma_1 &= 1/2(\phi_1+\phi_2) & \epsilon_1 &= 1/2(\psi_1+\psi_2) \\ \gamma_2 &= 1/2(\phi_2+\phi_3) & \epsilon_2 &= 1/2(\psi_2+\psi_3) \\ \gamma_3 &= 1/2(\phi_3+\phi_1) & \epsilon_3 &= 1/2(\psi_3+\psi_1) \end{aligned} \tag{6}$$

be defined. Then when α and β assume the values

$$\begin{aligned} \alpha &= \pi - \gamma_N & \beta &= \pi - \epsilon_N \\ \alpha &= 2\pi - \gamma_N & \beta &= \pi - \epsilon_N \\ \alpha &= \pi - \gamma_N & \beta &= 2\pi - \epsilon_N \\ \alpha &= 2\pi - \gamma_N & \beta &= 2\pi - \epsilon_N \\ &\text{For } N = 1,\ 2, \text{ or } 3 \end{aligned} \tag{7}$$

the terms NUM1, NUM2, and DENOM are all equal to zero. This means that K_1 and K_2 given by Eq. (4) are indeterminate. The significance of these special points will be discussed later in the paper.

MECHANISM MAPPING IN $\alpha\beta$ PLANE

We seek $\alpha\beta$ values which produce the result

$$\lambda_1 > 0 \qquad \lambda_3 > 0 \qquad \lambda_4 > 0$$

$$\text{and } \lambda = \frac{(\lambda_1 + \lambda_3 + \lambda_4)}{\sqrt{3}} > \frac{\sqrt{3}}{3} \tag{8}$$

If DENOM > 0, then NUM1 and NUM2 must also be greater than zero. If DENOM < 0, then NUM1 and NUM2 must also be less than zero. The regions in the plane where Eq. (8) is satisfied can therefore be investigated by finding the locations where NUM1, NUM2, and DENOM are zero. These loci will separate the regions where each of the terms are greater than zero from the regions where this is not the case.

Locus of NUM1 = 0

When NUM1 = 0 this corresponds to the condition that

$$(B_1-B_2)(C_2-C_3) = (B_2-B_3)(C_1-C_2). \tag{9}$$

Letting

$$\begin{array}{ll} D_1 = \sin 1/2(\psi_1-\psi_2) & D_5 = \sin 1/2(\psi_2-\psi_3) \\ D_2 = \sin 1/2(\phi_2-\phi_3-\psi_2+\psi_3) & D_6 = \sin 1/2(\phi_1-\phi_2-\psi_1+\psi_2) \\ D_3 = 1/2(\psi_1+\psi_2) & D_7 = 1/2(\psi_2+\psi_3) \\ D_4 = 1/2(\phi_2+\phi_3-\psi_2-\psi_3) & D_8 = 1/2(\phi_1+\phi_2-\psi_1-\psi_2) \end{array} \tag{10}$$

the locus where NUM1 = 0 is defined by

$$\tan\alpha = \frac{D_1D_2\sin(D_3+\beta)\sin(D_4-\beta)-D_5D_6\sin(D_7+\beta)\sin(D_8-\beta)}{D_5D_6\sin(D_7+\beta)\cos(D_8-\beta)-D_1D_2\sin(D_3+\beta)\cos(D_4-\beta)}. \tag{11}$$

For each value of α found from Eq. (11), Eq. (9) will also be satisfied if π is added to or subtracted from the value of α.

Locus of NUM2 = 0

When NUM2 = 0 this corresponds to the condition that

$$(A_1-A_2)(C_2-C_3) = (A_2-A_3)(C_1-C_2). \tag{12}$$

Letting

$$\begin{array}{ll} E_1 = 1/2(\phi_1-\phi_2) & E_5 = 1/2(\phi_2-\phi_3) \\ E_2 = \sin 1/2(\phi_1-\phi_2) & E_6 = \sin 1/2(\phi_2-\phi_3) \\ E_3 = \sin 1/2(\phi_3-\phi_2-\psi_3+\psi_2) & E_7 = \sin 1/2(\phi_2-\phi_1-\psi_1-\psi_2) \\ E_4 = 1/2(\phi_2+\phi_3-\psi_2-\psi_3 & E_8 = 1/2(\phi_1+\phi_2-\psi_1-\psi_2) \end{array} \tag{13}$$

the locus where NUM2 = 0 is defined by

$$\tan\beta = \frac{E_6E_7\sin(E_5+\alpha)\sin(E_8+\alpha)-E_2E_3\sin(E_1+\alpha)\sin(E_4+\alpha)}{E_6E_7\sin(E_5+\alpha)\cos(E_8+\alpha)-E_2E_3\sin(E_1+\alpha)\cos(E_4+\alpha)}. \tag{14}$$

For each value of β found from Eq. (14), Eq. (12) will also be satisfied if π is added to or subtracted from the value of β.

Locus of DENOM = 0

When DENOM = 0 this corresponds to the condition

$$(A_1-A_2)(B_2-B_3) = (A_2-A_3)(B_1-B_2). \tag{15}$$

Letting

$$\begin{array}{ll} F_1 = \sin 1/2(\phi_1-\phi_2) & F_5 = \sin 1/2(\phi_2-\phi_3) \\ F_2 = \sin 1/2(\psi_2-\psi_3) & F_6 = \sin 1/2(\psi_1-\psi_2) \\ F_3 = 1/2(\psi_2+\psi_3) & F_7 = 1/2(\psi_1+\psi_2) \\ F_4 = 1/2(\phi_1+\phi_2) & F_8 = 1/2(\phi_2+\phi_3) \end{array} \tag{16}$$

the locus where DENOM = 0 is defined by

$$\tan\beta = \frac{F_1F_2\sin(F_4+\alpha)\sin F_3-F_5F_6\sin(F_8+\alpha)\sin F_7}{F_5F_6\sin(F_8+\alpha)\cos F_7-F_1F_2\sin(F_4+\alpha)\cos F_3}. \tag{17}$$

Again, the β values found from Eq. (17) may be shifted by adding or subtracting π and still satisfy Eq. (15).

NUMERICAL EXAMPLE

In order to illustrate the appearance of the loci defined by Eqs. 11, 14, and 17 a numerical example was chosen where

$$\begin{array}{ll} \phi_1 = 22° & \psi_1 = 12° \\ \phi_2 = 76° & \psi_2 = 34° \\ \phi_3 = 134° & \psi_3 = 78° \end{array} \tag{18}$$

Fig. 2 shows the result of using these values in Eq. (11). The regions where NUM1 < 0 are labelled with a minus and those where NUM1 > 0 are labelled with a plus. The division between these regions is the locus computed from Eq. (11). Figs. 3 and 4 show the results for NUM2 and DENOM with the same labelling procedures.

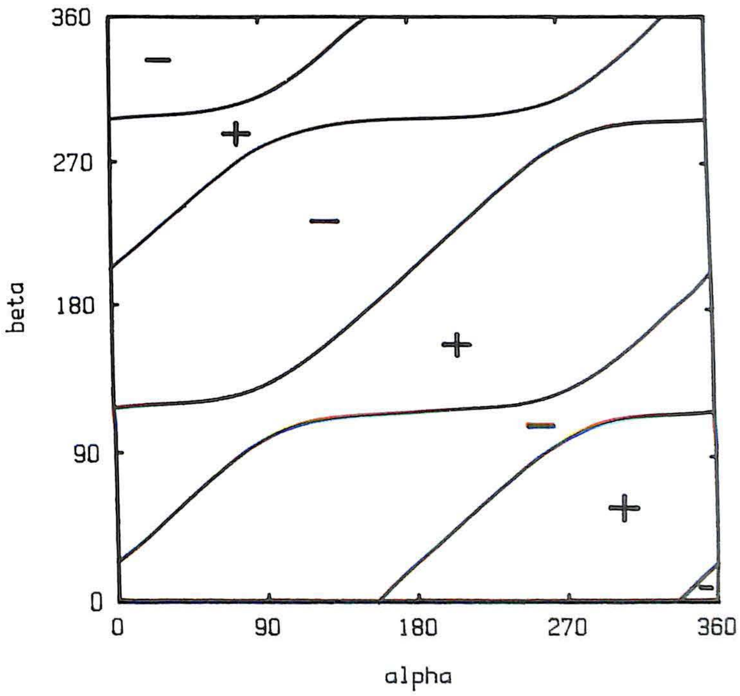

Fig. 2 Locus of NUM1 = 0 in $\alpha\beta$ Plane

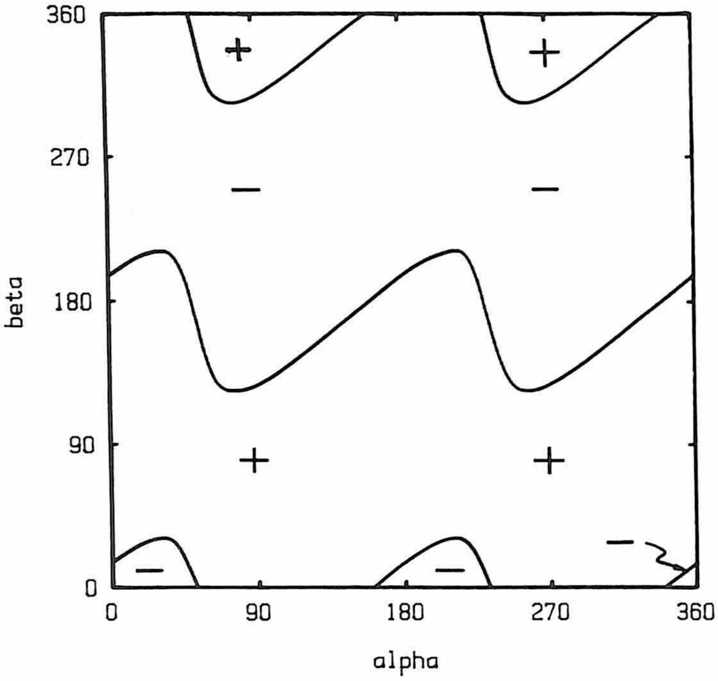

Fig. 3 Locus of NUM2 = 0 in $\alpha\beta$ Plane

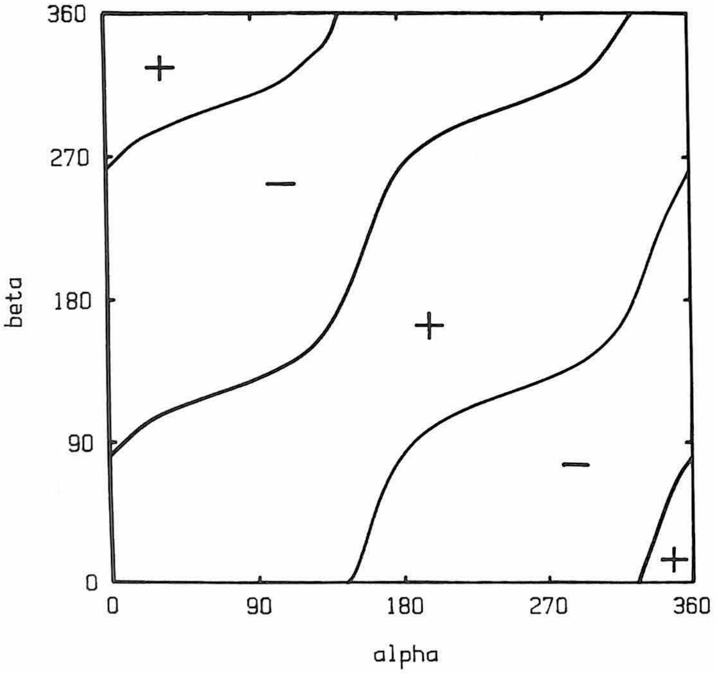

Fig. 4 Locus of DENOM = 0 in $\alpha\beta$ Plane

Superposition of Regions

If all of the regions from Figs. 2, 3, and 4 where NUM1, NUM2, and DENOM are all positive are added to those regions where they are all three negative, the map shown in Fig. 5 will result. The shaded region corresponds to $\alpha\beta$ choices which satisfy the conditions given by Eq. (8). The regions which are not shaded need not be considered since the design specifications given in Eq. (18) cannot be satisfied with $\alpha\beta$ choices which lie in these areas.

Change Point Boundaries

The shaded region of Fig. 5 represents two infinities of solutions to the function generation problem defined by the data given in Eq. (18). With this large number of solutions to choose from, any additional information about the characteristics of the mechanisms which satisfy Eq. (18) would be helpful in making the final selection. The region shown in Fig. 5 where a solution does exist can be subdivided into regions where eight particular categories of planar

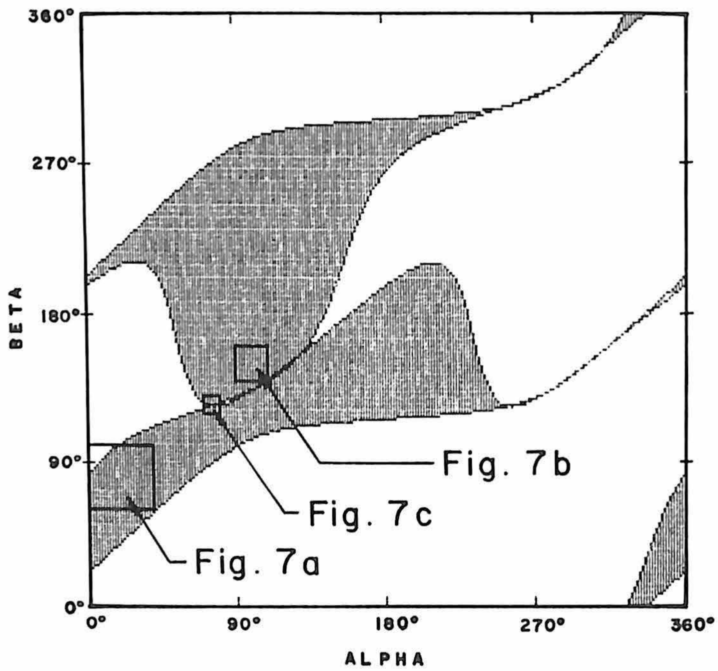

Fig. 5 Regions Where a Solution Exists for Numerical Example

four bar mechanisms as proposed by Barker [1] occur by considering the change point conditions. For example, when the link lengths are such that

$$1 + \lambda_1 = \lambda_3 + \lambda_4 \tag{19}$$

then Eq. (2) takes the form

$$\begin{aligned} K_1(A_1+1)+K_2(B_1+1) &= 1-C_1 \\ K_1(A_2+1)+K_2(B_2+1) &= 1-C_2 \\ K_1(A_3+1)+K_2(B_3+1) &= 1-C_3. \end{aligned} \tag{20}$$

Solving for K_1 and K_2 from the first pair of equations and substituting into the third yields

$$(A_3+1)[(1-C_2)(B_1+1)-(1-C_1)(B_2+1)] \\ -(B_3+1)[(A_1+1)(1-C_2)-(A_2+1)(1-C_1)] \\ -(1-C_3)[(A_2+1)(B_1+1)-(A_1+1)(B_2+1)] = 0 \tag{21}$$

which contains only α and β. It is therefore possible to choose a value for α and solve numerically for the corresponding β's which satisfy Eq. (21). This procedure was followed for the numerical example given by Eq. (18) and the locus defined by Eq. (19) plotted as shown in Fig. 6.

The other two change point conditions occur when

$$1 + \lambda_3 = \lambda_1 + \lambda_4$$

and (22)

$$1 + \lambda_4 = \lambda_1 + \lambda_3$$

and the locus for these can be found in a similar fashion. However, the results can also be obtained directly from Fig. 6 simply by in one case shifting each point shown in Fig. 6 by π in β, and in the other case by π in both α and β. When all three change point loci are superimposed on the regions shown in Fig. 5 the result is a complete map of the $\alpha\beta$ plane showing where each type of mechanism exists. It is possible that one or more mechanisms will not appear in the map because there may be none of this type which can satisfy the three position specifications.

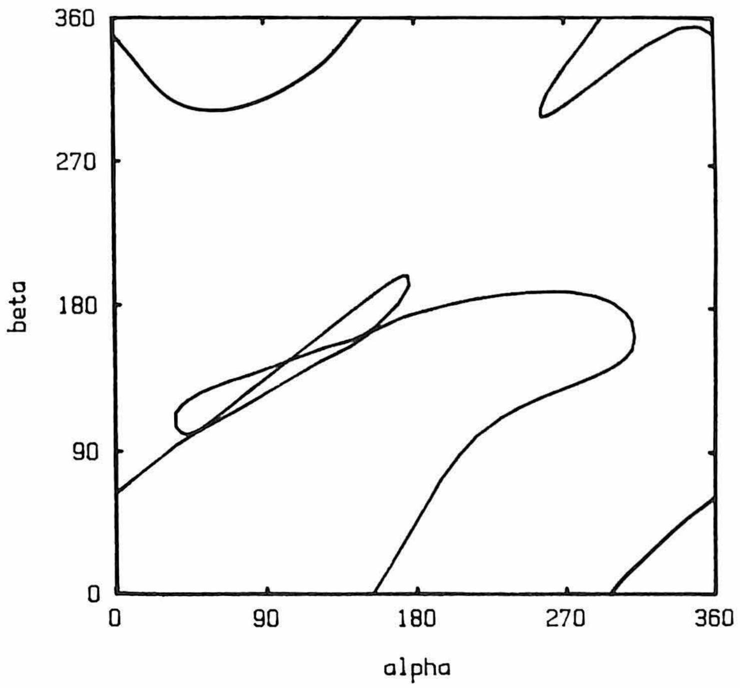

Fig. 6 Locus of Change Point $1 + \lambda_1 = \lambda_3 + \lambda_4$

EXAMINATION OF PARTICULAR REGIONS IN THE $\alpha\beta$ PLANE

Particular regions of the full map may be examined to illustrate how the choice of α and β influences the result. For example in Fig. 7a the range of α is 0° to 40° while the range of β is 60° to 100°. As shown these choices result in mechanisms which are either GCRR, GRCR, RRR1 or RRR4. The regions are subdivided by two change point boundaries and at the intersection of these boundaries a double change point mechanism is found which satisfies the function generation problem. This point in Fig. 7a is labelled "DBCP" and for the data of Eq. (18) corresponds to the result

$$\alpha = 20.8686°$$
$$\beta = 81.6223°$$
$$\lambda_1 = 1.4577$$
$$\lambda_3 = 1.000$$
$$\lambda_4 = 1.4577.$$

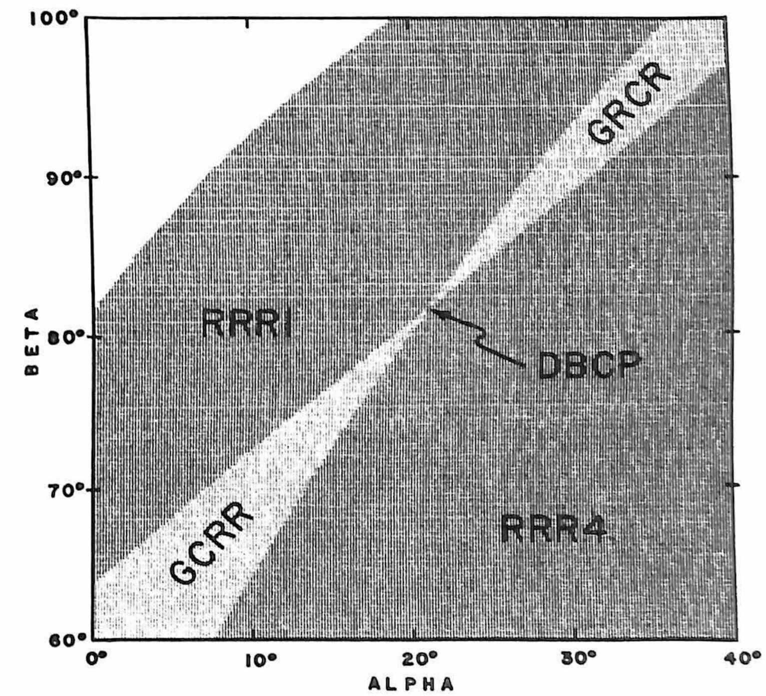

Fig. 7a Example of Double Change Point Location

Fig. 7b shows the region where α has the range 90° to 110° and β has the range 140° to 160°. In this case the region is again subdivided by two change point boundaries one of which intersects itself. At this intersection a false double change point occurs where

$$\alpha = 180 - \phi_2 = 104°$$
$$\beta = 180 - \psi_2 = 146°$$
$$\lambda_1 = .727$$
$$\lambda_3 = .265$$
$$\lambda_4 = 1.462.$$

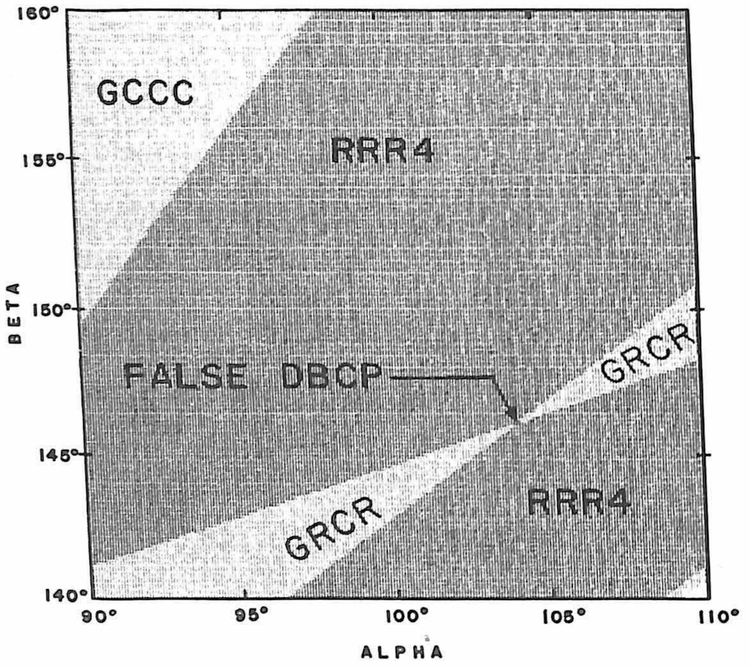

Fig. 7b Example of False Double Change Point Location

Fig. 7c shows the region 70° $< \alpha <$ 80° and 120° $< \beta <$ 130°. This region contains one of the indeterminate points defined by Eqs. (6) and (7) which for the data of Eq. (18) places the point at α = 75°, β = 124°. All three of the change point boundaries pass through this special indeterminate point. In addition, the angle of approach to the indeterminate point determines the value of the λ_1, λ_3, and λ_4 and consequently of λ itself. This means that a wide range of contours of constant λ can be expected to pass through the indeterminate points.

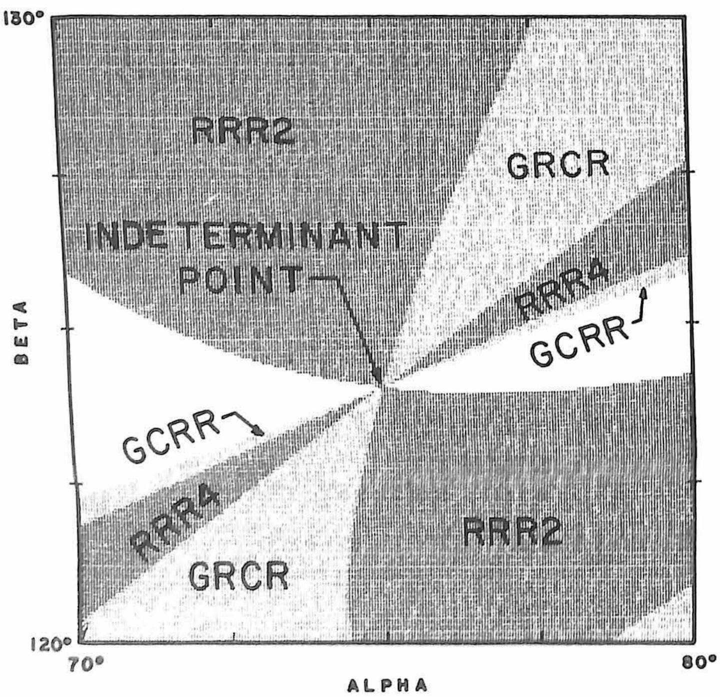

Fig. 7c Example of Indeterminate Point Location

CONTOURS OF CONSTANT λ

Contours of constant λ add additional information to the $\alpha\beta$ map of the function generation problem. Also if a contour of constant λ can be constructed in the $\alpha\beta$ plane, then this contour can be transformed into a trace in the equivalent λ plane of the solution space. This makes it possible to relate all of the previous work done by Barker on characteristic surfaces for mechanism properties to the present work [2,3,4].

The condition $\lambda = (\lambda_1+\lambda_3+\lambda_4)/\sqrt{3}$ equals a chosen constant is the same as saying that

$$3K_1\lambda^2 + 2\sqrt{3}\lambda(K_1K_2+K_2) + 2K_2^2 + 2K_2K_3 - K_1 = 0. \quad (23)$$

Then eliminating K_3 and using Eq. (4) it is possible to show that

$$\begin{aligned}&3\lambda^2(\mathrm{NUM1})(\mathrm{DENOM}) + 2(\mathrm{NUM2})^2(1-B_1)\\ &-2(\mathrm{NUM2})(\mathrm{DENOM})(\sqrt{3}\lambda-C_1) - (\mathrm{NUM1})(\mathrm{DENOM}) \quad (24)\\ &-2(\mathrm{NUM1})(\mathrm{NUM2})(\sqrt{3}\lambda-A_1) = 0\end{aligned}$$

Eq. (24) contains only α, β, and λ so that for a chosen λ it is possible to solve numerically for $\alpha\beta$ pairs which satisfy Eq. (24). This procedure was followed to construct Fig. 8 in which the λ = 4 contour is shown. The three crosses shown are some of the special indeterminate points predicted by Eq. (7), and as predicted the λ = 4 contour passes through these locations. Fig. 9 was drawn using the λ = 4 contour data from Fig. 8 and represents the location in the solution space of all the mechanisms which satisfy this function generation problem and in addition possess a λ of four.

Starting at point A in Fig. 9 it can be seen that at this location the mechanism type would correspond to a RRR3. Moving along the trace to B a change point occurs so that from B to C all the mechanisms are GCRR's. Fig. 8 shows the corresponding points and point C happens to be close to the location β = 0° or β = 360°. From C to D in Fig. 9 the trace is in the RRR1 region and then changes back into the GCRR zone from D to E. From E to F it is again RRR1 and then from F to G once again become GCRR. By continuing on from point to point in Fig. 9 (and the corresponding points in Fig. 8) the trace of λ = 4 eventually connects back to the starting point of A.

Fig. 9 provides a great deal of useful information which can be integrated with previous developments regarding the solution space. For example, if a solution is desired in which the input link is a crank,

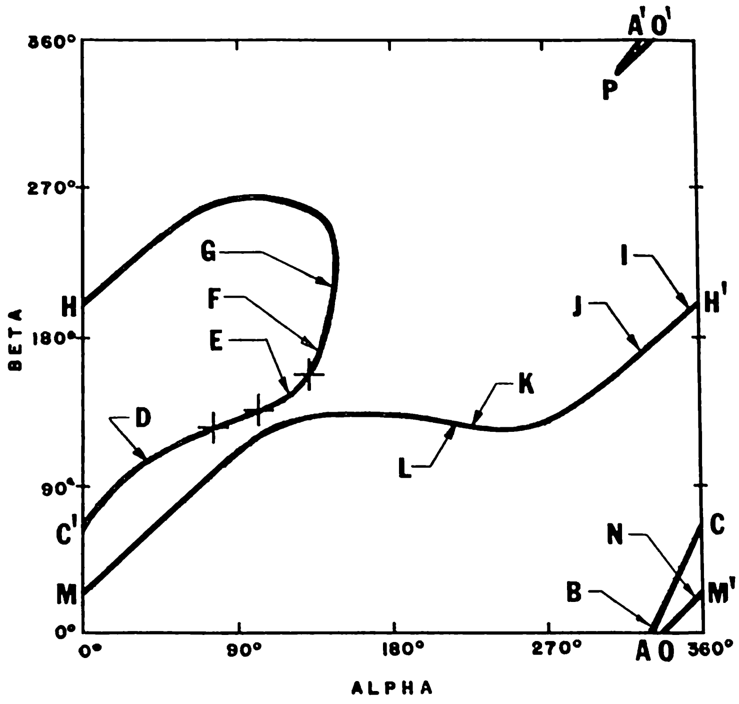

Fig. 8 Contour of $\lambda = 4$ in $\alpha\beta$ Plane

then only those locations in Fig. 9 in the GCCC and GCRR regions need be considered. However, the trace in the GCCC region is veryclose to the change point boundaries and consequently the transmission angle of these mechanisms would come close to having a minimum of 0° and a maximum of 180°. This leaves as potential solutions the portion of the trace between B&C and between F&G. Some of these mechanisms would have

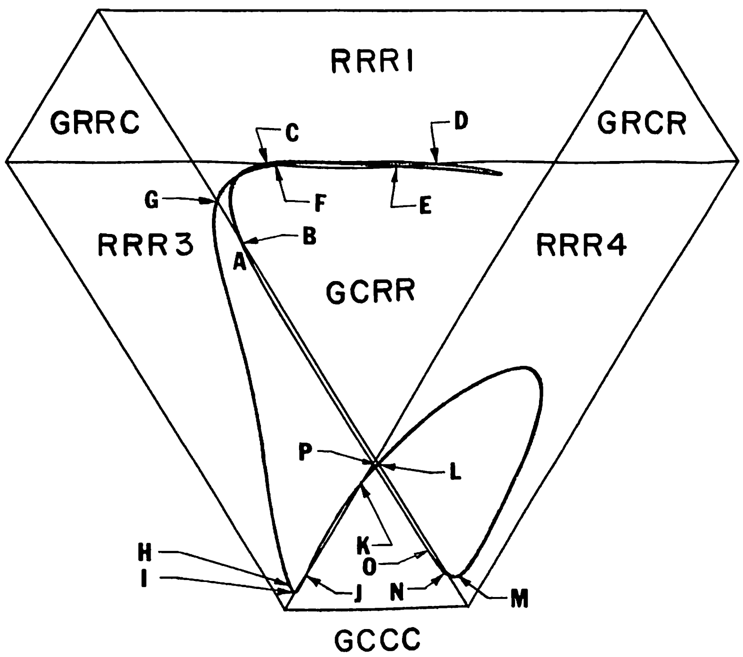

Fig. 9 Contour of $\lambda = 4$ in Solution Space

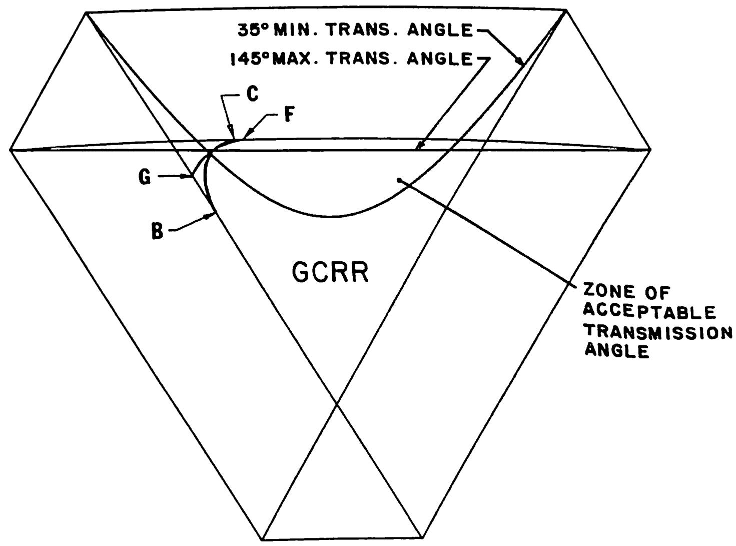

Fig. 10 Acceptable Transmission Angle Region in $\lambda = 4$ Plane

reasonable transmission angles since as shown in Fig. 10 a zone of favorable transmission angles with the minimum being greater than 35° and the maximum being less than 145° intersects with the traces BC and FG from the previous figure [2].

TYPICAL SOLUTIONS

In order to illustrate typical solutions to the synthesis problem, two points were chosen on the $\lambda = 4$ contour of Fig. 9 in the GCRR region.

Solution One:

$$\alpha = 142.984°$$
$$\beta = 193.333°$$
$$\lambda_1 = 2.859$$
$$\lambda_3 = 2.783$$
$$\lambda_4 = 1.286$$
$$\lambda = 4.0$$

When this mechanism is assembled in Form Two the transmission angle will have the range -33.9° to -140.1° and the output angle has the range -52.4° to -154.7°.

Solution Two:

$$\alpha = 344.200°$$
$$\beta = 31.481°$$
$$\lambda_1 = 2.784$$
$$\lambda_3 = 2.844$$
$$\lambda_4 = 1.300$$
$$\lambda = 4.0$$

When this mechanism is assembled in Form One the transmission angle will have the range 26.9° to 127.9° and the output angle will have the range 42.5° to 146.6°.

For both these solutions it is easy to show that the design positions given by Eq. (18) are satisfied simply by adding α and β to the ϕ's and ψ's respectively for the three precision positions.

CONCLUSION

The synthesis task of three position function generation for a planar four bar mechanism has been considered. Two infinities of solutions are possible since the reference positions defined by the angles α and β may be chosen. The effects of α and β on determining the type of planar four bar have been considered by mapping the $\alpha\beta$ plane according to the classification scheme proposed by Barker. The $\alpha\beta$ plane is partitioned into subregions by the change point conditions. Useful information to assist in making the final selection of the synthesis problem can be obtained by generating contours of constant λ in the $\alpha\beta$ plane and also in the solution space. With these contours it is possible to not only satisfy the function generation specifications, but also select solutions which exhibit additional desirable characteristics.

REFERENCES

1. Barker, C. R., "A Complete Classification of Planar Four-Bar Linkages", Mechanism and Machine Theory, Vol. 20, No. 6, pp. 535-554, 1985.
2. Barker, C. R., "Characteristic Surfaces in the Solution Place of Planar Four Bar Mechanisms", Part 1 ASME Paper 84-DET-126, Part 2 ASME Paper 84-DET-127, 1984.
3. Barker, C. R., and Ywh-Ren Jeng, "Range of the Six Fundamental Position Angles of a Planar Four Bar Mechanism", Mechanism and Machine Theory, Vol. 20, No. 4, pp. 329-344, 1985.
4. Barker, C. R., "Characteristic Surfaces for Extreme Values of Angular Velocity Ratio in Planar Four Bar Mechanisms", accepted for publication in Mechanism and Machine Theory.
5. Waldron, K. J., and R. T. Strong, "Improved Precision Position Mechanism Synthesis", Report No. Tr-12, Department of Mechanical Engineering, University of Houston, October 1978.
6. Gupta, K. C., "A General Theory for Synthesizing Crank-Type Four Bar Function Generators with Transmission Angle Control", Journal of Applied Mechanisms, Vol. 45, No. 2, June 1968.
7. Harber, M. T., A. G. Erdman, and D. R. Riley, "Enhanced Computer Graphic Kinematic Synthesis for Three Prescribed Positions", Proceedings of CAD/CAM, Robotics and Automation International Conference, February 13-15, 1985, Tuscon, Arizona.
8. Harber, M. T., A. G. Erdman, and D. R. Riley, "Lincages Package Enhancement: A New Method of Three Design Position Synthesis", Proceedings of the 9th Applied Mechanisms Conference, October 28-30, 1985, Kansas City, Missouri.
9. Freudenstein, F., "An Analytical Approach to the Design of Four-Link Mechanisms", Transactions of the ASME, 76, pp. 483-492, 1954.